

Supplementary Materials for

Complete three-dimensional structures of the Lon protease translocating a protein substrate

Shanshan Li, Kan-Yen Hsieh, Chiao-I Kuo, Szu-Hui Lee,
Grigore D. Pintilie, Kaiming Zhang*, Chung-I Chang*

*Corresponding author. Email: kmzhang@ustc.edu.cn (K.Z.); chungi@gate.sinica.edu.tw (C.-I.C.)

Published 15 October 2021, *Sci. Adv.* **7**, eabj7835 (2021)
DOI: 10.1126/sciadv.abj7835

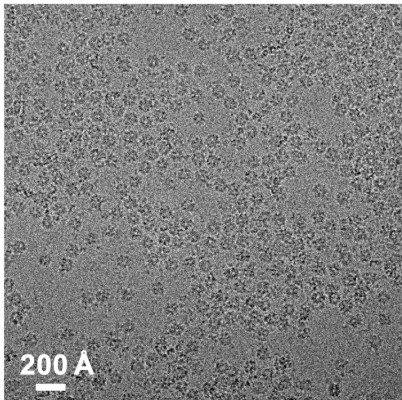
The PDF file includes:

Figs. S1 to S6
Legends for movies S1 and S2
Tables S1 and S2

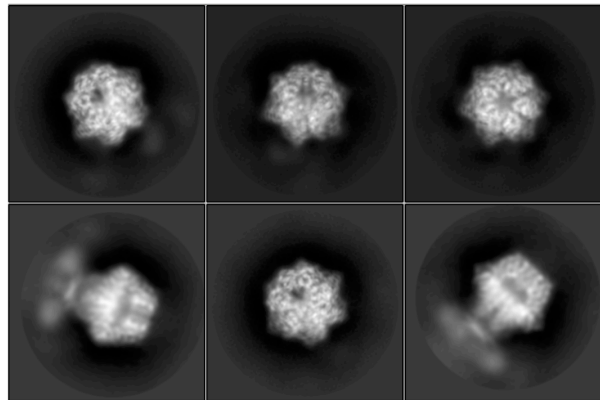
Other Supplementary Material for this manuscript includes the following:

Movies S1 and S2

A



B



C

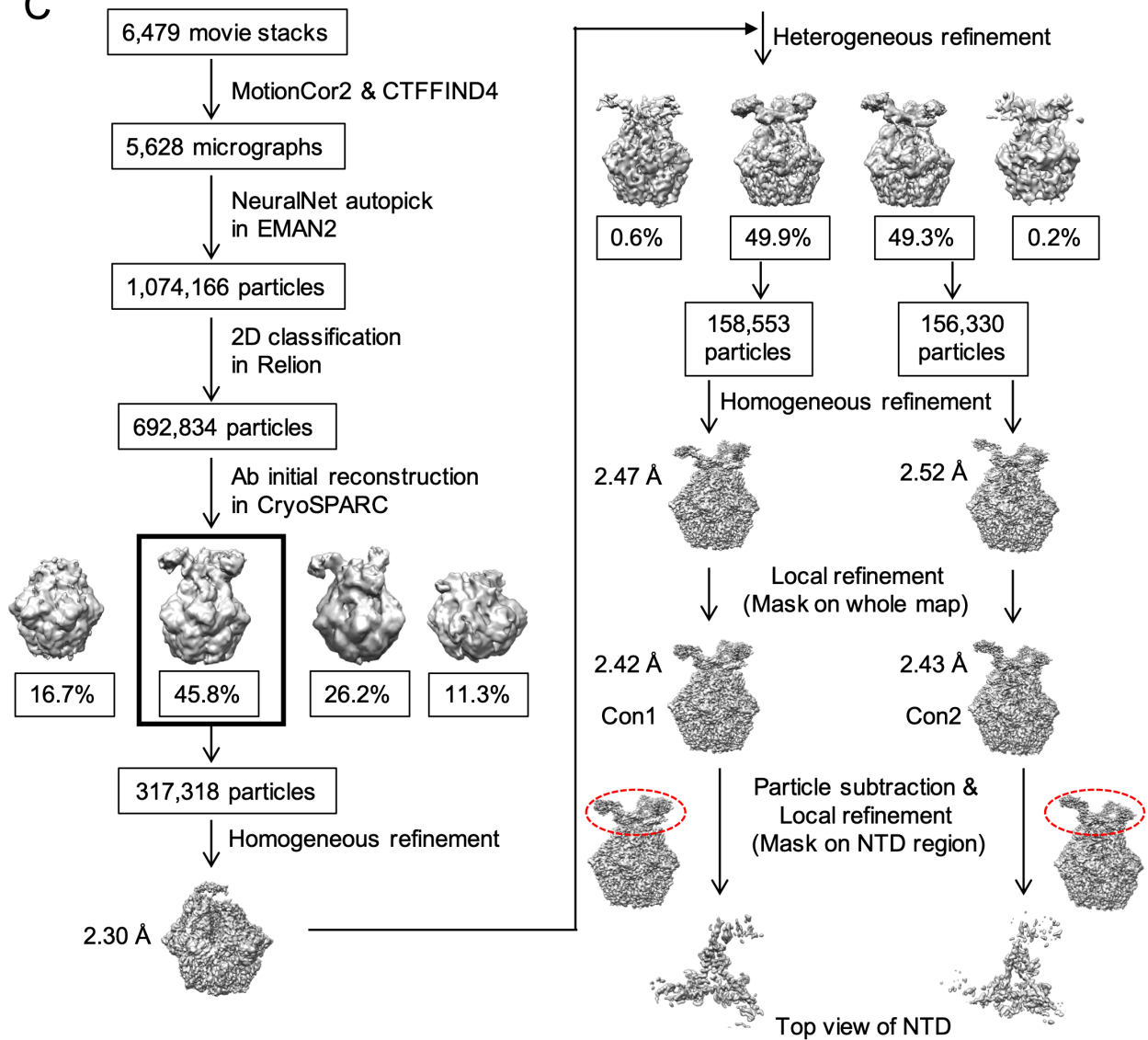


Fig. S1. Single-particle cryo-EM analysis of substrate-engaged MtaLon. (A) Representative motion-corrected cryo-EM micrograph. (B) Reference-free 2D class averages. (C) Workflow of the data processing.

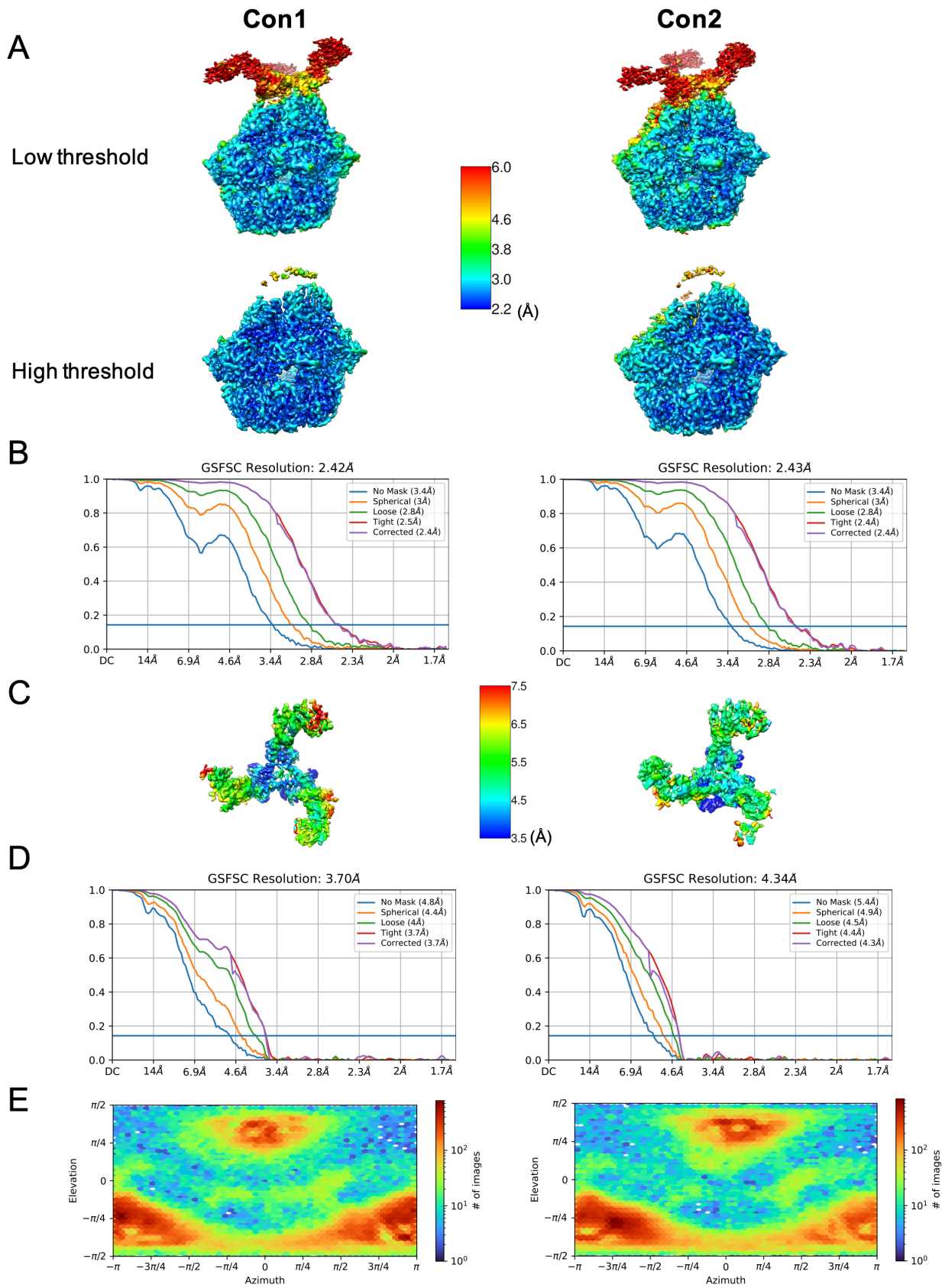


Fig. S2. Evaluation of the final 3D reconstructions of substrate-engaged MtaLon. (A)

Resolution maps for the final 3D reconstructions of Con1 (left) and Con2 (right), shown at two different thresholds. **(B)** Gold standard FSC plots for the 3D reconstructions of Con1 (left) and Con2 (right), calculated in cryoSPARC. **(C)** Resolution maps for the 3D reconstructions of NTD from Con1 (left) and Con2 (right). **(D)** Gold standard FSC plots for the 3D reconstructions of NTD from Con1 (left) and Con2 (right). **(E)** Euler angle distribution of the particle images.

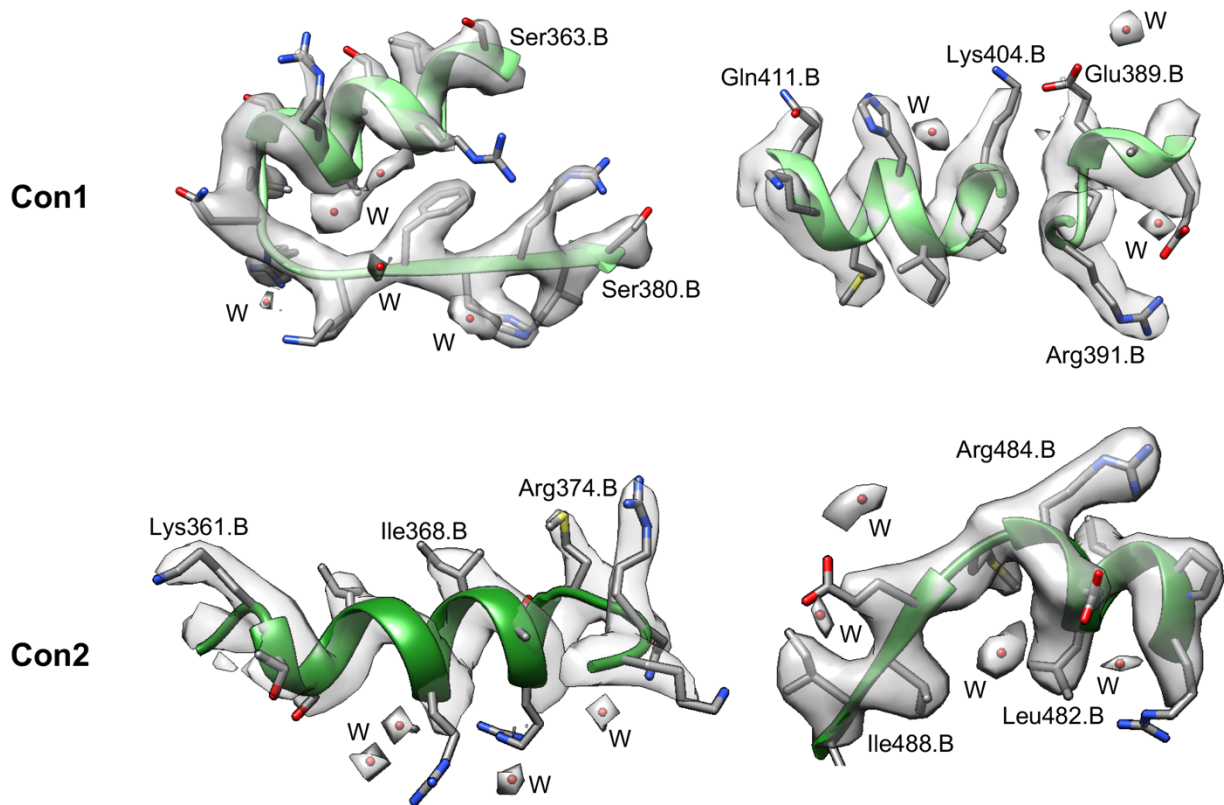


Fig. S3. Selected regions of the high-resolution maps showing good resolvability for water molecules. The model is shown as ribbon, with water molecules (W) indicated. Some side chains, shown in sticks, are labelled by residue name and number, followed by the chain ID.

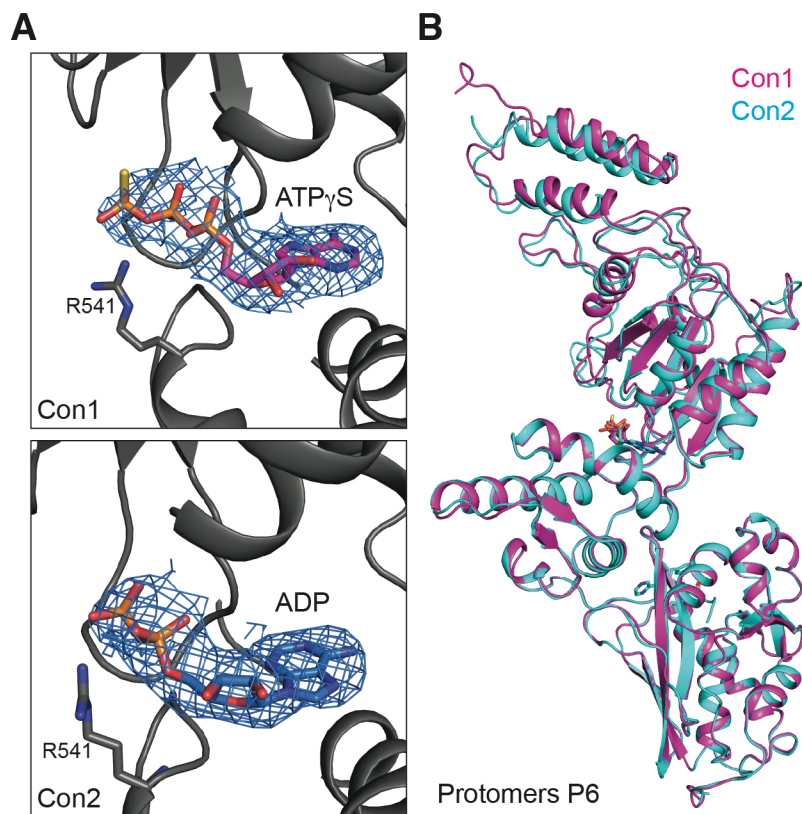


Fig. S4. Nucleotide binding in the non-engaging protomer P6. (A) Cryo-EM maps, contoured at 5.15σ , and molecular model of the bound nucleotide in the non-engaging protomers P6 (chain F) in Con1 (ATP γ S; top) and Con2 (ADP; bottom) structures. The sensor-II residue Arg541 is also shown. (B) Superimposition of the structures of the P6 protomers in Con1 and Con2, with an RMSD value of 1.09 \AA , based on C α atoms of residues 245-780.

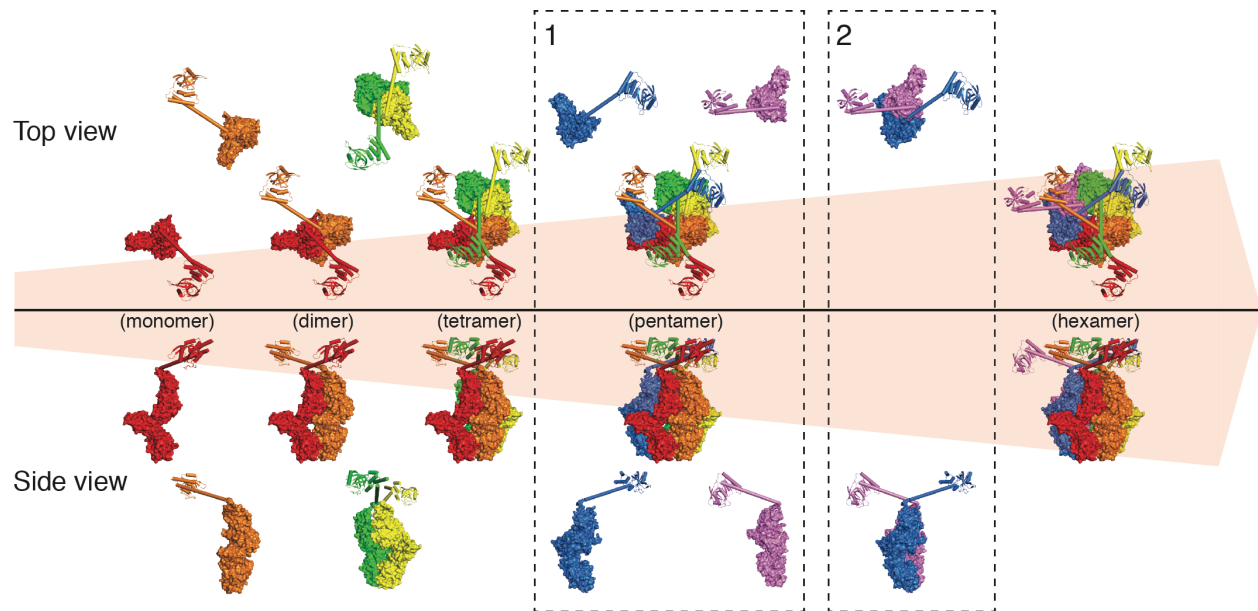


Fig. S5. Proposed model for the sequential assembly of Lon protein complex. Schematic diagram showing assembly of a Lon homo-hexamer with interlocked N-terminal helices. The proposed process involves monomers and Ac-Ob-paired dimers. Surface representations of the protomers with rainbow coloring (from red to violet) are used to depict a sequential assembly, which proceeds from left to right as denoted by the background light pink arrow. The numbered dashed boxes represent two alternative pathways to assembling a hexamer from a tetramer.

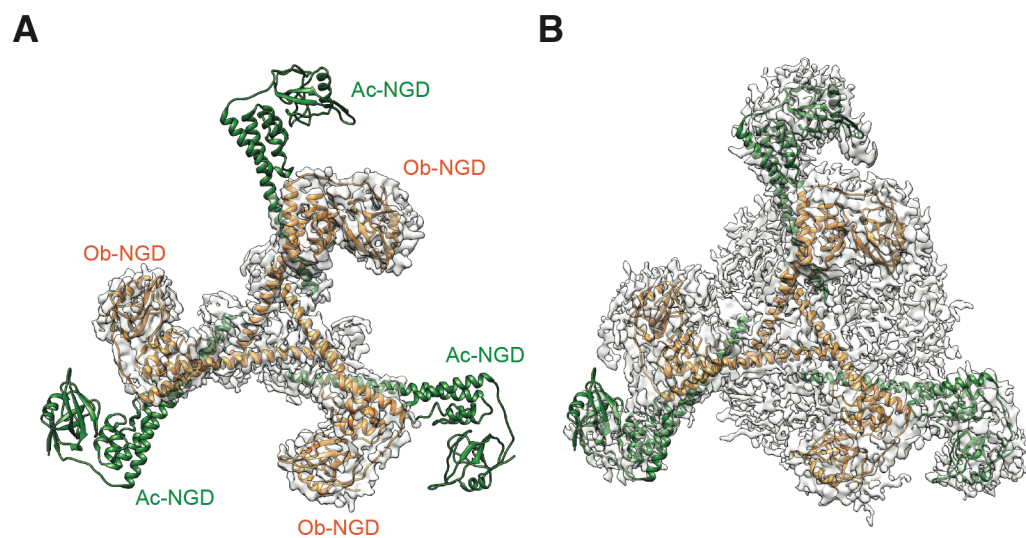


Fig. S6. The flexibility of the six N-terminal globular domains (NGDs). (A) Top view of the model and the focused refined map, with contour threshold value 0.35, showing the three flexible Ob-NGDs. (B) Top view of the model and the map, with contour threshold value 0.15, showing the location of three highly flexible Ac-NGDs.

Movie S1. Main features of cryo-EM Map1 and the reconstructed structure of Con1. The map and structure are shown to emphasize the features of full-length *Meiothermus taiwanensis* Lon protease (LonA) bound to α -casein.

Movie S2. Conformational changes associated with the ATP-hydrolysis cycle of full-length ATP-dependent Lon (LonA). The movie shows how the conformational states associated with the ATPase cycles are extrapolated based on the cryo-EM structures of Con1 and Con2 with bound α -casein, and how the conformational movement may drive substrate translocation.

Table S1. Cryo-EM data collection, processing, and model validation

	MtaLon
Data collection and processing	
Microscope	Titan Krios G3i
Voltage (kV)	300
Camera	Thermo Fisher Falcon 4
Grids Type	R1.2/1.3 Quantifoil copper grid (200 mesh)
Sample concentration	0.5 mg/mL
Magnification	96,000×
C2 aperture size (μm)	50
Objective aperture size (μm)	100
Pixel size (\AA)	0.82
Total exposure ($\text{e}^-/\text{\AA}^2$)	48
Exposure time (s)	5.8
Number of frames per exposure	40
Energy filter slit width (eV)	N/A
Data collection software	EPU 2.7
Maximum image shift (μm)	6
Number of exposures per hole	6

Defocus range (μm)	-0.5 - -1.7	
Number of micrographs collected	6,479	
Number of micrographs used	5,628	
Number of initial particles	1,074,166	
Conformations	Con1	Con2
Symmetry	C1	C1
Number of final particles	158,553	156,330
Resolution (0.143 gold standard FSC, \AA)	2.4	2.4
Local resolution range (\AA)	2 - 6	2 - 6
Atomic model refinement		
Software	phenix.real_space_refine	phenix.real_space_refine
Clashscore, all atoms	6.05	5.96
Poor rotamers (%)	0.38	0.41
Favored rotamers (%)	96.87	96.26
Ramachandran outliers (%)	0.30	0.24
Ramachandran favored (%)	93.27	93.50
MolProbity score	1.77	1.75
Bad bonds (%)	0.03	0.04
Bad angles (%)	0.12	0.09

Table S2. Primer list for site-directed mutagenesis

Primer Name	Sequence (5' to 3')
MtaLonA_M217A_F	CAG CGG GTC AAA GAA CAG GCG GAC ACC AAC CAG CGC GAG
MtaLonA_M217A_R	CTC GCG CTG GTT GGT GTC CGC CTG TTC TTT GAC CCG CTG
MtaLonA_M217S_F	CAG CGG GTC AAA GAA CAG TCG GAC ACC AAC CAG CGC GAG
MtaLonA_M217S_R	CTC GCG CTG GTT GGT GTC CGA CTG TTC TTT GAC CCG CTG
MtaLonA_M217L_F	CAG CGG GTC AAA GAA CAG CTG GAC ACC AAC CAG CGC GAG
MtaLonA_M217L_R	CTC GCG CTG GTT GGT GTC CAG CTG TTC TTT GAC CCG CTG
MtaLonA_M217Y_F	CAG CGG GTC AAA GAA CAG TAC GAC ACC AAC CAG CGC GAG
MtaLonA_M217Y_R	CTC GCG CTG GTT GGT GTC GTA CTG TTC TTT GAC CCG CTG
MtaLonA_Q221A_F	GAA CAG ATG GAC ACC AAC GCG CGC GAG TAC TAC CTG CGC
MtaLonA_Q221A_R	GCG CAG GTA GTA CTC GCG CGC GTT GGT GTC CAT CTG TTC
MtaLonA_Y224A_F	GAC ACC AAC CAG CGC GAG GCC TAC CTG CGC GAA CAG
MtaLonA_Y224A_R	CTG TTC GCG CAG GTA GGC CTC GCG CTG GTT GGT GTC

MtaLonA_Y224S_F	GAC ACC AAC CAG CGC GAG AGC TAC CTG CGC GAA CAG ATG AAG
MtaLonA_Y224S_R	CTT CAT CTG TTC GCG CAG GTA GCT CTC GCG CTG GTT GGT GTC
MtaLonA_Y224I_F	GAC ACC AAC CAG CGC GAG ATT TAC CTG CGC GAA CAG ATG AAG
MtaLonA_Y224I_R	CTT CAT CTG TTC GCG CAG GTA AAT CTC GCG CTG GTT GGT GTC
MtaLonA_Y224L_F	GAC ACC AAC CAG CGC GAG CTC TAC CTG CGC GAA CAG ATG
MtaLonA_Y224L_R	CAT CTG TTC GCG CAG GTA GAG CTC GCG CTG GTT GGT GTC
MtaLonA_Y224H_F	GAC ACC AAC CAG CGC GAG CAC TAC CTG CGC GAA CAG ATG
MtaLonA_Y224H_R	CAT CTG TTC GCG CAG GTA GTG CTC GCG CTG GTT GGT GTC
MtaLonA_Y224M_F	GAC ACC AAC CAG CGC GAG ATG TAC CTG CGC GAA CAG ATG
MtaLonA_Y224M_R	CAT CTG TTC GCG CAG GTA CAT CTC GCG CTG GTT GGT GTC
MtaLonA_Y224F_F	GAC ACC AAC CAG CGC GAG TTC TAC CTG CGC GAA CAG ATG
MtaLonA_Y224F_R	CAT CTG TTC GCG CAG GTA GAA CTC GCG CTG GTT GGT GTC

MtaLonA_Y224W_F	GAC ACC AAC CAG CGC GAG TGG TAC CTG CGC GAA CAG
MtaLonA_Y224W_R	CTG TTC GCG CAG GTA CCA CTC GCG CTG GTT GGT GTC
MtaLonA_Y225A_F	ACC AAC CAG CGC GAG TAC GCC CTG CGC GAA CAG ATG AAG
MtaLonA_Y225A_R	CTT CAT CTG TTC GCG CAG GGC GTA CTC GCG CTG GTT GGT
MtaLonA_Y225S_F	ACC AAC CAG CGC GAG TAC AGC CTG CGC GAA CAG ATG AAG
MtaLonA_Y225S_R	CTT CAT CTG TTC GCG CAG GCT GTA CTC GCG CTG GTT GGT
MtaLonA_Y225L_F	ACC AAC CAG CGC GAG TAC CTC CTG CGC GAA CAG ATG AAG
MtaLonA_Y225L_R	CTT CAT CTG TTC GCG CAG GAG GTA CTC GCG CTG GTT GGT
MtaLonA_L226A/M230A_F	CGC GAG TAC TAC GCG CGC GAA CAG GCG AAG GCC ATC CAG
MtaLonA_L226A/M230A_R	CTG GAT GGC CTT CGC CTG TTC GCG CGC GTA GTA CTC GCG
MtaLonA_M230A/I233A/L237A_F	GAA CAG GCG AAG GCC GCC CAG AAA GAG GCG GGT GGC GAG GAT G
MtaLonA_M230A/I233A/L237A_R	CAT CCT CGC CAC CCG CCT CTT TCT GGG CGG CCT TCG CCT GTT C
MtaLonA_L205A/V209A/V213A/M217A_F	GCT GAT AAA AGG GCC GCC CAG CGG GCC AAA GAA CAG GCG GAC ACC AAC CA

MtaLonA_L205A/V209A/V213A/
M217A_R

GCC TGT TCT TTG GCC CGC TGG GCG GCC CTT TTA TCA GCC
TCG AAG CGC TC